Theoretical predictions of arsenic and selenium species under atmospheric conditions

MaryTheresa Monahan-Pendergast, Michelle Przybylek,
Mark Lindblad, Jennifer Wilcox*

Department of Chemical Engineering, Worcester Polytechnic Institute, 100 Institute Road, Worcester, MA 01609, USA

Abstract

Thermochemical properties of arsenic and selenium species thought to be released into the atmosphere during the coal combustion were examined using ab initio methods. At various levels of theory, calculated geometries and vibrational frequencies of the species were compared with experimental data, where available. Through a comparison of equilibrium constants for a series of gaseous arsenic and selenium oxidation reactions involving OH and HO_2, five thermodynamically favored reactions were found. In addition, it was determined that all favored reactions were more likely to go to completion under tropospheric, rather than stratospheric, conditions.

1. Introduction

Globally, coal combustion provides a major source of energy with more than five billion short tons of coal burned each year (Katzer, 2007). In the United States, approximately 52% of electricity comes from coal, an amount expected to increase in the coming decades (Energy Information Administration (EIA), 2005; Katzer, 2007). As the use of coal for power increases, attention turns to the potentially harmful effects associated with its combustion. Along with the well-known problem of CO_2 emissions, various trace elements are emitted. When coal combusts, both arsenic and

selenium are volatilized and escape the smokestacks either as a gas or enriched in the fly ash (Senior et al., 2000). Both trace elements naturally occur in the earth's crust; however, at high concentrations they can have adverse effects on the environment and human health. By understanding the speciation and lifetime of arsenic and selenium in the atmosphere, technologies can be developed to better deal with these potentially harmful elements.

Arsenic ranks 20th in trace elements found in the earth's crust (National Research Council (NRC), 1997). Natural cycles, such as weathering and volcanic activity, emit arsenic into the atmosphere (Cullen and Reimer, 1989); however, studies have traced nearly 75% of arsenic emissions to anthropogenic sources (Zeng et al., 2001). Arsenic content in coal averages 2 ppm (Commission on Life Sciences (CLS), 1977), making coal combustion

*Corresponding author. Tel.: +1 508 831 5493; fax: +1 508 831 5853.

E-mail address: jwilcox@wpi.edu (J. Wilcox).

a major source of anthropogenic arsenic release (Han et al., 2003). When arsenic species enter drinking water sources humans may suffer arsenic toxicity, symptoms of which include problems of the gastrointestinal tract, circulatory system, immune system, and renal system. Skin lesions and cancers, particularly Bowen's disease, may also result (Duker et al., 2005). To protect drinking water sources it is important to look at the lifetime of arsenic species in the atmosphere, i.e., whether they enter the stratosphere, are flushed out with rainwater, or adsorb onto dust particles and settle into soil. Arsenic exists in two oxidation states, the trivalent As(III) and pentavalent As(V). As(III) molecules, such as $AsCl_3$ and AsH_3, tend to be water-soluble (Hudson-Edwards et al., 2005; Efermov et al., 2002). The species As_2, As_4, and elemental As are also found to be at least partially water-soluble (Young, 1979; Harrington et al., 1997). If these molecules are stable in the atmosphere, they will likely end up in soil or fresh water. Arsenic (V) molecules tend to be prone to adsorption (Frentiu et al., 2007) and will likely make their way into soil by adsorbing onto dust or soot particulates.

Selenium levels in coal average 1 ppm (Shah et al., 2007), making coal combustion the main source of anthropogenic release of selenium (ATSDR, 2003). As with arsenic, selenium uptake by humans can be toxic, but, unlike arsenic, selenium plays an essential role as an antioxidant enzyme (Tinggi, 2003). The lower recommended daily intake of selenium is $55\,\mu g\,day^{-1}$ for adults (ATSDR, 2003). Diet provides most of the necessary selenium, preventing against the health effects of selenium deficiencies such as Keshan and Kashin–Beck diseases, which cause cardiovascular and joint problems, respectively. On the other hand, over-consumption of selenium, i.e., intake levels greater than $400\,\mu g\,day^{-1}$, can lead to selenium toxicity, known as selenosis. Symptoms of selenosis include dermal effects such as loss of hair and nails as well as neurological effects such as numbness and paralysis (ATSDR, 2003). In addition to these issues, high levels of selenium have led to birth defects in birds (Ohlendorf et al., 1986) and fish (Lemly, 1993). Although no selenium overdoses in humans have been directly linked to coal combustion emissions and the effects of selenium inputs into the ecosystem may not be immediately noticeable, selenium inputs from coal emissions need to be monitored since excess selenium can be difficult to remove (Lemly, 1997). The varying species of selenium may have

different fates in the environment. For instance, selenium dioxide is water-soluble (Zhang, 2002), and can be dissolved in rainwater when released into the atmosphere. Also, species such as elemental Se and SeO_2 can condense at low temperatures and readily adsorb onto particles (Yan, 2004). Through their deposition onto soil or vegetation, they have a direct path into the food chain when such soil or vegetation is consumed. Certain plants, such as *Astragalus bisulcatus*, are known to accumulate selenium in their leaves, causing toxicities in grazing animals (Pickering et al., 2000). Knowledge of selenium's speciation will allow scientists to monitor selenium by predicting its final form, where it is deposited, and, ultimately, its effects on the environment.

Previous experimental and theoretical work on the arsenic and selenium species that may be released from coal combustion was used to determine the possible species that may exist as reactants in the atmosphere. By combusting coal, Senior and Bool concluded that both arsenic and selenium are vaporized in the combustion process. The vapors then condense onto fly ash particles during cooling or remain in gaseous form (Senior et al., 2000). Yan et al. (1999) completed equilibrium modeling through minimizing the Gibbs free energy of the system likely to determine the composition of arsenic, selenium, and mercury species released from coal combustion. The species, AsO, $AsCl_3$, AsH_3, As_2, As_4, H_2Se, SeO, SeO_2, $SeCl_2$, and elemental Se were all found to be possible stable species in the flue gases of coal combustion. Yan et al. later performed combustion simulations confirming the existence of Se, SeO, and SeO_2 in combustion flue gases (Yan et al., 2001, 2004). Thermodynamic modeling was also carried out by Miller et al. (2003) to determine the speciation of trace elements in coal combustion where As_4O_{10}, As_4O_7, As_4O_6, As_4O_8, AsO, and AsO_2 were found to be probable emission species. From these predicted species, As, AsO, Se, and SeO were chosen for atmospheric oxidation reaction calculations via OH and HO_2 radical species. Although these investigations provide insight into the possible arsenic and selenium species that are released from coal combustion processes, they provide no insight into the atmospheric lifetime of these pollutants once released from the stacks. The current investigation involves an examination of the atmospheric cycle of these species generated from coal combustion flue gases.

Theoretical calculations were carried out to enhance the knowledge of gaseous arsenic and selenium speciation within the atmosphere. Beginning with an investigation of the theoretical thermochemical data for several key reactions allows for increased understanding of the pathway of anthropogenic arsenic and selenium cycling through the biosphere. According to Molina et al. (1996), the free radicals OH and HO_2 play a major role in determining the lifetimes of various compounds in the atmosphere. For this reason, this work focuses on the oxidation of As and Se species by OH and HO_2 to then determine the relative stabilities of the oxidized forms of these species. Once these oxidized forms are recognized it can be determined how they might cycle through the biosphere, i.e., through rainwater, particulates, soil, freshwater, etc. For instance, understanding the oxidation pathways of As and Se species to the potentially water-soluble forms, As, As(III)O, As(III)O_2, and SeO_2, will be crucial in the development of effective control technologies.

2. Computational methodology

Calculations were carried out using the Gaussian 03 suite of programs (Frisch et al., 2004). Basis sets incorporating relativistic effects for the inner electrons were explored through the use of small core relativistic effective core potentials (RECP) for arsenic and selenium. This basis set employs the relativistic ECP28MWB pseudopotential of the Stuttgart group (Martin and Sundermann, 2001) for both arsenic and selenium, with the respective energy-optimized (4s2p)/[3s2p] and (4s5p)/[2s3p] Gaussian-type orbital (GTO) valence bases optimized using multiconfiguration Dirac–Fock (MCDF) calculations. The second basis set employs a relativistic compact effective potential, RCEP28VDZ of Stevens and Krauss (1992), which replaces 28 of arsenic's and 28 of selenium's atomic core electrons, derived from numerical Dirac–Fock wavefunctions using an optimizing process based upon the energy-overlap functional. Energy-optimized (5s5p)/[2s2p] Gaussian type double-ς quality sp and triple-ς quality d functions were used, with the triple-ς d functions essential for describing the orbital shape changes that exist with d occupancy. Although both of these basis sets were employed for As and Se species in the basis set justification, through a balance of accuracy and computational expense, just the ECP28MWB pseudopotential of the

Stuttgart group was used for As and a complete Pople basis set for Se. More specifically, a comparison of the theoretical predictions from the pseudopotentials to those of a complete basis set was carried out with the complete basis set calculations performed using the 6-311G* basis set. This extended triple-zeta Pople basis set, which includes an additional polarization function, was used for selenium, hydrogen, and oxygen.

3. Basis set justification

To determine the most accurate level of theory, six arsenic and selenium species were evaluated using four methods: CCSD, CCSD(T), QCISD, and QCISD(T) combined with each of the Pople basis sets: 6-311G, 6-311 + G, 6-311G*, and 6-311 + G*, as well as the Stevens ECP and ECP28MWB pseudopotential of the Stuttgart group. The resulting vibrational frequencies were compared to experimental values in order to find the level of theory with the lowest absolute error. The accurate prediction of the vibrational frequencies of the species in a system also closely predicts the energy of the system, which is crucial for the calculation of thermodynamic and kinetic properties. The QCISD level of theory along with the 6-311G* basis set was chosen for all species except those containing arsenic, for which the ECP28MWB pseudopotential of the Stuttgart group was selected.

3.1. Vibrational frequency comparison

Table 1 presents computed vibrational frequencies along with experimental values. From the comparison of the vibrations, the best level of theory was chosen. When compared with experiment, QCISD/6-311G* performed well (within 20 wavenumbers) for all selenium species. Most of the arsenic species were too computationally intensive to run without ECPs. When compared with experimental values, QCISD with the ECP28MWB pseudopotential of the Stuttgart group performed well for all arsenic species. The selenium species were also less computationally intensive with the ECPs, but reduced computation time did not compensate for the greatly reduced accuracy. At the chosen level of theory, comparison between predicted theoretical vibrational frequencies and available experimental literature data shows an average absolute error of 14 wave numbers.

Table 1
Calculated and experimental vibrational frequencies (in cm^{-1})

Species	Vibrational mode	Experimental (cm^{-1})	Level of theory											
			QCISD						QCISD(T)					
			6-311G	6-311+G*	6-311G*	6-311+G	ECP28MWB	RCEP28DVZ	6-311G	6-311+G*	6-311G*	6-311+G	ECP28MWB	RCEP28DVZ
AsO	Stretch	967.08[a]	792.07	920.32	931.42	778.68	931.42	798.47	835.43	909.51	916.51	826.11	820.91	793.03
AsO$_2$	Bend		213.21	235.94	233.01	213.98	220.29	220.26	209.65	227.34	224.31	209.83	214.24	214.45
	Asym. stretch		441.91	515.85	520.92	430.78	448.35	501.39	440.46	497.45	503.74	430.11	477.19	490.76
	Sym. stretch		558.50	606.61	615.97	545.69	581.81	583.45	553.28	593.27	604.19	538.57	572.33	574.22
AsOH	Se-stretch		642.80	679.03	691.65	630.46	651.26	652.43	646.41	668.28	683.75	631.11	643.43	644.88
	Bend		1048.99	1035.57	1060.63	1003.63	1079.64	1086.17	1041.34	1019.04	1044.82	994.62	1066.86	1072.51
	H-stretch		3629.46	3801.98	3810.37	3629.41	3829.18	3819.55	3608.41	3762.87	3775.15	3605.43	3794.91	3784.87
SeO	Stretch	907.1[b]	644.08	892.71	894.40	684.61	696.85	632.96	747.75	855.24	857.07	741.68	780.36	779.29
SeO$_2$	Sym. stretch	920.8	729.29	915.72	924.52	711.45	779.38	752.38	688.87	858.38	863.80	678.83	724.91	698.78
	Bend	369.8[c]	320.09	359.94	365.09	315.08	333.68	319.59	306.24	344.92	349.42	301.58	314.44	300.98
	Asym. stretch	968[c]	718.57	956.05	972.32	678.86	797.67	773.00	725.79	911.02	924.00	704.20	754.81	729.11
SeOH	Se-stretch		583.97	642.78	648.00	577.54	605.04	609.30	591.18	631.48	639.13	581.67	599.34	603.88
	Bend		1141.52	1131.03	1154.00	1098.64	1183.59	1180.10	1139.39	1119.46	1144.62	1093.77	1174.66	1170.31
	H-stretch		3595.37	3794.09	3805.00	3591.82	3822.39	3811.80	3575.76	3753.98	3766.08	3571.04	3788.53	3778.34
			Level of theory											
			CCSD						CCSD(T)					
			6-311G	6-311+G*	6-311G*	6-311+G	ECP28MWB	RCEP28DVZ	6-311G	6-311+G*	6-311G*	6-311+G	ECP28MWB	RCEP28DVZ
AsO	Stretch	967.08[a]	888.85	982.39	991.52	878.77	892.05	863.15	828.23	918.91	926.99	815.96	830.35	801.15
AsO$_2$	Bend		221.26	242.40	239.27	222.46	226.74	226.37	212.87	230.23	227.36	213.53	217.16	217.37
	Asym. stretch		467.84	531.58	535.85	459.15	509.40	524.89	447.59	500.43	506.49	439.23	483.72	499.30
	Sym. stretch		569.53	612.04	621.44	557.12	589.82	593.00	558.78	594.59	605.96	545.71	576.08	579.36
AsOH	As-Stretch		673.61	698.93	713.34	658.24	669.40	672.16	653.63	674.74	691.56	638.51	651.13	653.34
	Bend		1054.71	1042.71	1067.94	1008.83	1084.80	1092.78	1041.31	1020.76	1046.79	996.68	1068.07	1074.01
	H-stretch		3656.34	3817.94	3825.77	3657.67	3845.08	3836.97	3614.72	3767.96	3780.15	3610.63	3799.49	3790.75
SeO	Stretch	907.1[b]	766.05	900.60	902.36	762.77	792.51	781.00	765.25	863.03	864.65	761.96	791.56	791.04
SeO$_2$	Sym. stretch	920.8	791.38	949.48	958.88	774.22	819.96	795.29	720.99	876.78	883.10	709.41	749.61	723.88
	Bend	369.8[c]	335.87	367.98	373.02	331.63	344.00	332.25	314.17	347.71	352.54	309.74	320.71	306.69
	Asym. stretch	968[c]	849.34	995.75	1011.70	821.91	867.17	854.18	770.40	927.02	939.45	750.45	786.08	767.29
SeOH	Se-stretch		609.18	657.20	664.15	599.26	620.84	626.88	599.60	638.44	646.93	589.46	611.05	619.70
	Bend		1151.44	1138.73	1161.99	1109.29	1189.46	1187.54	1141.52	1122.61	1148.21	1096.66	1177.27	1173.74
	H-stretch		3621.20	3808.55	3819.45	3616.33	3835.82	3823.67	3580.97	3759.49	3769.79	3576.97	3793.71	3784.27

[a]CRC: Handbook of Chemistry and Physics (1989).
[b]Herzberg (1951).
[c]Thermodynamics Source Database (2005).

Table 2
Calculated and experimental bond lengths (in Å) and bond angles (in deg)

Species	Multiplicity	Bond length (Å) Bond angle (deg)	Experimental (cm^{-1})	Level of theory											
				QCISD						QCISD(T)					
				6-311G	6-311+G*	6-311G*	6-311+G	ECP28MWB	RCEP28DVZ	6-311G	6-311+G*	6-311G*	6-311+G	ECP28MWB	RCEP28DVZ
AsO	2	r(AsO)	1.6236[a]	1.6841	1.6429	1.6402	1.6872	1.6582	1.679	1.6856	1.6511	1.6488	1.6876	1.6702	1.691
AsO$_2$	4	r(AsO)		1.8626	1.8051	1.8013	1.8691	1.8434	1.8621	1.8657	1.8098	1.8044	1.875	1.8492	1.8685
		θ(OAsO)		94.1467	94.4906	95.2085	93.8874	93.8	92.7825	94.0916	94.8469	95.6537	93.9954	93.8879	92.7778
		r(AsO)		1.8048	1.7876	1.7821	1.8106	1.8085	1.8283	1.8066	1.7946	1.7875	538.57	1.8145	1.8345
AsOH	1	r(AsH)		0.9739	0.9636	0.9623	0.9749	0.9603	0.9613	0.9752	0.966	0.9645	1.8136	643.43	0.9634
		θ(HAsO)		117.5964	112.5412	111.3402	119.6615	113.0106	111.9744	117.5985	112.0955	110.868	0.9765	0.9624	111.7078
		r(SeO)	1.6393[b]	1.7376	1.6562	1.6553	1.7338	1.7081	1.733	1.7362	1.6685		1.6678	119.6741	112.7406	1.72817
SeO	3	r(SeO)	1.6076	1.6899	1.6181	1.6153	1.6953	1.6581	1.6799	1.7104	1.6349	1.6324	1.7376	1.7074	1.7059
SeO$_2$	1	r(SeO)	1.6076	1.6899	1.6181	1.6153	1.6953	1.6581	1.6799	1.7101	1.6347	1.6321	1.715	1.6817	1.7051
		θ(OSeO)	113.83[b]	113.8029	114.9009	115.3377	113.2295	112.7909	112.2824	113.9851	115.0381	115.5018	1.7138	1.6817	112.5123
		r(OSe)		1.8605	1.8147	1.811	1.8647	1.8446	1.8649	1.861	1.8221	1.8175	113.4376	112.9692	1.8713
SeOH	2	r(OH)		0.9774	0.9646	0.9631	0.9785	0.9616	0.9624	0.9786	0.9671	0.9655	1.8668	0.9636	0.9644
		θ(SeOH)		111.5314	108.7592	107.8408	112.9491	108.7771	108.0415	111.5207	108.3043	107.3245	112.9583	108.5153	107.7946

Species	Multiplicity	Bond length (Å) Bond angle (deg)	Experimental (cm^{-1})	Level of theory											
				CCSD						CCSD(T)					
				6-311G	6-311+G*	6-311G*	6-311+G	ECP28MWB	RCEP28DVZ	6-311G	6-311+G*	6-311G*	6-311+G	ECP28MWB	RCEP28DVZ
AsO	2	r(AsO)	1.6236[a]	1.6641	1.6309	1.6286	1.6661	1.6469	1.6647	1.6846	1.648	1.6457	1.6869	1.6676	1.6881
AsO$_2$	4	r(AsO)		1.8616	1.8069	1.803	1.8679	1.845	1.8629	1.8644	1.8085	1.8037	1.872	1.8485	1.8675
		θ(OAsO)		93.6754	93.9162	94.655	93.3543	93.3441	92.3857	93.9709	94.6187	95.4081	93.7963	93.695	92.6192
		r(AsO)		1.7942	1.7805	1.7751	1.7999	1.8019	1.821	1.8038	1.7924	1.785	1.8101	1.8117	1.8314
AsOH	1	r(AsH)		0.9723	0.9627	0.9614	0.9732	0.9594	0.9603	0.9749	0.9657	0.9642	0.9762	0.9622	0.9631
		θ(HAsO)		118.2008	112.8775	111.7264	120.1959	113.3445	112.3205	117.8124	112.2459	111.0292	119.7875	112.9204	111.8922
SeO	3	r(SeO)	1.6393[b]	1.7237	1.6533	1.6528	1.7244	1.6959	1.7165	1.7324	1.6663	1.6658	1.7338	1.7047	1.7252
SeO$_2$	1	r(SeO)	1.6076	1.6734	1.6109	1.608	1.6782	1.6473	1.6676	1.7012	1.6306	1.628	1.7056	1.6747	1.6983
		r(SeO)	1.6076	1.6734	1.6109	1.608	1.6782	1.6473	1.6676	1.7005	1.6304	1.6277	1.7053	1.6746	1.6972
		θ(OSeO)	113.83[b]	113.4661	115.0367	115.4497	112.9533	112.6479	111.9309	113.7523	115.0436	115.4979	113.2175	112.8108	112.2926
SeOH	2	r(OSe)		1.8491	1.8085	1.8048	1.8546	1.8387	1.859	1.8579	1.8193	1.8146	1.8634	1.8474	1.8672
		r(OH)		0.9757	0.9637	0.9623	0.977	0.9608	0.9618	0.9783	0.9667	0.9653	0.9795	0.9633	0.964
		θ(SeOH)		112.0128	108.9926	108.097	113.3361	109.0086	108.269	111.672	108.4186	107.4138	113.1059	108.6689	107.9572

[a] Evenson et al. (1970) and Mizushima (1972).
[b] CRC: Handbook of Chemistry and Physics (1989).

3.2. Equilibrium geometry comparison

Table 2 presents the computed geometries along with available experimental values. Calculated arsenic to oxygen bond lengths among all levels considered in this study overpredict the experimental distance by 0.0424 Å on average. At the chosen level of theory for arsenic, specifically for the AsO species, the absolute error from the experimental value is 0.0346 Å. A similar analysis for the SeO species reveals an absolute error of 0.016 Å, while the average selenium to oxygen bond length, over all levels investigated, is over predicted by 0.0634 Å. All levels of theory suggest a bent arrangement for the AsO_2 and SeO_2, which is consistent with experimental findings. Correlation between the computed values at the chosen levels of theory against experimental data confirmed the chosen levels of theory worked well for these species.
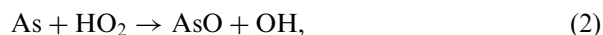
Table 3
Reaction enthalpies, entropies, and equilibrium constants of arsenic and selenium reactions

Reaction	Parameter	Units	Temperature (K)					
			223.15	253.15	298.15	400	500	600
(a) Arsenic reactions								
$As + OH \rightarrow AsOH$	ΔH	kcal mol^{-1}	−29.71	−29.81	−29.94	−30.18	−30.36	−30.49
	ΔS	cal mol K^{-1}	−24.47	−24.87	−25.35	−26.06	−26.46	−26.71
	K_{eq}	–	5.65 (23)	1.99 (20)	2.54 (16)	6.25 (10)	3.08 (7)	1.87 (5)
$As + HO_2 \rightarrow AsO + OH$	ΔH	kcal mol^{-1}	−22.94	−22.90	−22.84	−22.72	−22.62	−22.55
	ΔS	cal mol K^{-1}	1.02	1.17	1.38	1.74	1.96	2.09
	K_{eq}	–	4.90 (22)	1.07 (20)	1.12 (17)	6.23 (12)	2.08 (10)	4.69 (8)
$As + OH \rightarrow AsO + H$	ΔH	kcal mol^{-1}	7.99	8.00	8.02	8.10	8.21	8.35
	ΔS	cal mol K^{-1}	−1.81	−1.77	−1.69	−1.46	−1.21	−0.96
	K_{eq}		6.05 (9)	5.13 (−8)	5.65 (−7)	1.80 (−5)	1.40 (−4)	5.61 (−4)
$AsO + HO_2 \rightarrow AsO_2 + OH$	ΔH	kcal mol^{-1}	43.58	43.68	43.82	44.14	44.42	44.65
	ΔS	cal mol K^{-1}	0.01	0.38	0.90	1.83	2.46	2.89
	K_{eq}	–	2.06 (−43)	2.37 (−38)	1.19 (−32)	1.91 (−24)	1.32 (−19)	2.31 (−16)
$AsO + OH \rightarrow AsO_2 + H$	ΔH	kcal mol^{-1}	74.51	74.57	74.68	74.96	75.25	75.55
	ΔS	cal mol K^{-1}	−2.84	−2.56	−2.16	−1.36	−0.71	−0.17
	K_{eq}	–	2.52 (−74)	1.14 (−65)	6.02 (−56)	5.52 (−42)	8.89 (−34)	2.77 (−28)
(b) Selenium reactions								
$Se + OH \rightarrow SeOH$	ΔH	kcal mol^{-1}	−51.14	−51.24	−51.38	−51.63	−51.81	−51.96
	ΔS	cal mol K^{-1}	−22.46	−22.87	−23.36	−24.08	−24.50	−24.76
	K_{eq}	–	1.53 (45)	1.76 (39)	3.61 (32)	8.83 (22)	1.97 (17)	3.27 (13)
$Se + HO_2 \rightarrow SeO + OH$	ΔH	kcal mol^{-1}	−25.07	−25.04	−24.98	−24.87	−24.78	−24.71
	ΔS	cal mol K^{-1}	2.37	2.51	2.72	3.03	3.24	3.36
	K_{eq}	–	1.18 (25)	1.46 (22)	4.02 (18)	1.79 (14)	3.46 (11)	5.45 (9)
$SeO + HO_2 \rightarrow SeO_2 + OH$	ΔH	kcal mol^{-1}	19.52	−19.48	−19.40	−19.25	−19.09	−18.95
	ΔS	cal mol K^{-1}	−5.78	−5.61	−5.33	−4.88	−4.53	−4.28
	K_{eq}		7.19 (17)	3.92 (15)	6.68 (12)	2.82 (9)	2.26 (7)	9.31 (5)
$Se + OH \rightarrow SeO + H$	ΔH	kcal mol^{-1}	5.83	5.84	5.86	5.93	6.03	6.16
	ΔS	cal mol K^{-1}	−0.46	−0.43	−0.36	−0.16	0.07	0.30
	K_{eq}	–	1.53 (−6)	7.31 (−6)	4.97 (−5)	5.30 (−4)	2.39 (−3)	6.63 (−3)
$SeO + OH \rightarrow SeO_2 + H$	ΔH	kcal mol^{-1}	11.38	11.40	11.44	11.56	11.72	11.92
	ΔS	cal mol K^{-1}	−8.61	−8.55	−8.40	−8.07	−7.70	−7.34
	K_{eq}	–	9.31 (−14)	1.96 (−12)	8.26 (−11)	8.36 (−9)	1.56 (−7)	1.33 (−6)

Numbers in parentheses indicate powers of 10.

4. Results and discussion

Table 3a and b present the reaction enthalpies, entropies, and equilibrium constants for a selection of gas phase reactions involving arsenic and selenium. Five As and Se oxidation reactions were found to be spontaneous, having negative Gibb's free energy changes:

$$As + OH \rightarrow AsOH, \qquad (1)$$

$$As + HO_2 \rightarrow AsO + OH, \qquad (2)$$

$$Se + OH \rightarrow SeOH, \qquad (3)$$

$$Se + HO_2 \rightarrow SeO + OH, \qquad (4)$$

$$SeO + HO_2 \rightarrow SeO_2 + OH. \qquad (5)$$

Of these, all were more likely to go to completion at tropospheric (lower) temperatures than at stratospheric (higher) temperatures. Graphs showing variations in K_{eq} over a range of temperatures appear in Figs. 1 and 2. For elemental arsenic, its oxidation pathway is more likely to be the formation of AsOH by OH in the troposphere and to be the formation of AsO by HO_2 in the stratosphere. For elemental selenium, its oxidation pathway is more likely to be oxidation by the OH radical forming SeOH than oxidation by the HO_2 radical forming SeO at all temperatures. For AsO, no oxidation pathways were thermodynamically favored. For SeO, oxidation by HO_2 was favored, whereas oxidation by OH was not thermodynamically favored. The reactions involving capture of the oxygen atom from the OH radical by As or Se were
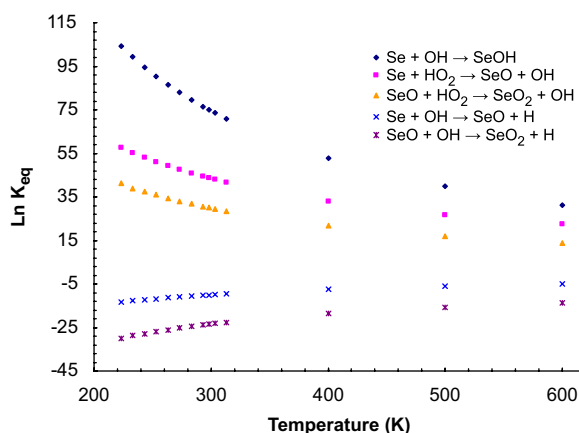

Fig. 2. Equilibrium constant plot for selenium reactions.

not thermodynamically favored. Equilibrium constants were evaluated over stratospheric pressures ranging from 0.2 to 1.0 atm; however, the order of magnitude of the equilibrium constants did not change with varying pressure. These thermodynamic calculations provide further understanding on the atmospheric speciation of arsenic and selenium species released from coal combustion processes. In future work a kinetic investigation will be carried out on the thermodynamically favored pathways to provide further insight into the atmospheric lifetimes of these coal combustion-generated pollutants.

5. Conclusions

Overall, the QCISD/6-311G* and QCISD with the ECP28MWB pseudopotential of the Stuttgart group performed best for all species and were used to calculate the energetics. From equilibrium constant calculations, possible oxidation–reduction mechanisms of As and Se compounds in the atmosphere were obtained. In particular, SeO_2 is water-soluble and the reaction between SeO and HO_2 may present a way for selenium from coal combustion to end up in drinking water. More work on arsenic and selenium remains. Kinetic studies need to be carried out on the thermodynamically favored reactions in order to find which reactions actually take place under atmospheric conditions. Once the thermodynamically and kinetically favored species of arsenic and selenium are determined, their properties, including water solubility and adsorption potential, must be fully understood

Fig. 1. Equilibrium constant plot for arsenic reactions.

so that the life cycle of these species can be traced through the biosphere.

Acknowledgments

References

Commission on Life Sciences (CLS), 1977. Arsenic: Medical and Biological Effects of Environmental Pollutants. National Academy of Sciences, Washington, DC.

Committee on Medical and Biological Effects of Environmental Pollutants. National Research Council (NRC), 1977. Arsenic: Medical and Biological Effects of Environmental Pollutants. The National Academies Press, Washington, DC.

Cullen, W., Reimer, K., 1989. Arsenic speciation in the environment. Chemical Reviews 89, 713–767.

Duker, A.A., Carranza, E.J.M., Hale, M., 2005. Arsenic geochemistry and health. Environmental International 31, 631–641.

Efermov, V.A., Potolokov, V.N., Nikolashin, S.V., Fedorov, V.A., 2002. Interaction of water with $GeCl_4$, $SnCl_4$, and $AsCl_3$. Inorganic Materials 38, 837–846 (translated from Neorganicheskie Materialy, 38, 996–1006).

Energy Information Administration (EIA), 2005. Basic Coal Statistics ⟨http://www.eia.doe.gov/neic/quickfacts/quickcoal.html⟩.

Evenson, K.M., Wells, J.S., Radford, H.E., 1970. Infrared resonance of OH with the water laser: a galactic maser pump? Physical Review Letters 25 (4), 199–202.

Frentiu, T., Vlad, S.-N., Ponta, M., Baciu, C. Kasler, I., Cordos, E., 2007. Profile distribution of As(III) and As(V) species in soil and groundwater in Bozanta area. Institute of Chemistry, Slovak Academy of Sciences.

Frisch, M.J., Trucks, G.W., Schlegel, H.B., Scuseria, G.E., Robb, M.A., Cheeseman, J.R., Montgomery Jr., J.A., Vreven, T., Kudin, K.N., Burant, J.C., Millam, J.M., Iyengar, S.S., Tomasi, J., Barone, V., Mennucci, B., Cossi, M., Scalmani, G., Rega, N., Petersson, G.A., Nakatsuji, H., Hada, M., Ehara, M., Toyota, K., Fukuda, R., Hasegawa, J., Ishida, M., Nakajima, T., Honda, Y., Kitao, O., Nakai, H., Klene, M., Li, X., Knox, J.E., Hratchian, H.P., Cross, J.B., Bakken, V., Adamo, C., Jaramillo, J., Gomperts, R., Stratmann, R.E., Yazyev, O., Austin, A.J., Cammi, R., Pomelli, C., Ochterski, J.W., Ayala, P.Y., Morokuma, K., Voth, G.A., Salvador, P., Dannenberg, J.J., Zakrzewski, V.G., Dapprich, S., Daniels, A.D., Strain, M.C., Farkas, O., Malick, D.K., Rabuck, A.D., Raghavachari, K., Foresman, J.B., Ortiz, J.V., Cui, Q., Baboul, A.G., Clifford, S., Cioslowski, J., Stefanov, B.B., Liu, G., Liashenko, A., Piskorz, P., Komaromi, I., Martin, R.L., Fox, D.J., Keith, T., Al-Laham, M.A., Peng, C.Y., Nanayakkara, A., Challacombe, M., Gill, P.M.W., Johnson, B., Chen, W., Wong, M.W., Gonzalez, C., Pople, J.A., 2004. Gaussian 03W, Version 6.1. Gaussian, Inc., Wallingford, CT.

Han, F.X., Su, Y., Monts, D.L., Plodinec, M.J., Banin, A., Triplett, G.E., 2003. Assesment of global industrial-age anthropogenic arsenic contamination. Naturwissenschaften 90, 395–401.

Harrington, C.F., Ojo, A.A., Lai, V.W.-M., Reimer, K.J., Cullen, W.R., 1997. The identification of some water-soluble arsenic species in the marine brown algae *Fucus distichus*. Applied Organometallic Chemistry 11, 931–940.

Herzberg, G., 1951. Molecular Spectra and Molecular Structure, I: Spectra of Diatomic Molecules. D. Van Nostrand Company, Inc., Princeton.

Hudson-Edwards, K.A., Jamieson, H.E., Charnock, J.M., Macklin, M.G., 2005. Arsenic speciation in waters and sediment of ephemeral floodplain pools, Ríos Agrio-Guadiamar, Aznalcóllar, Spain. Chemical Geology 219, 175–192.

Katzer, J., 2007. The Future of Coal: Options for a Carbon Constrained World. Massachusetts Institute of Technology (MIT), Boston, pp. 5–8.

Lemly, A.D., 1993. Teratogenic effects of selenium in natural populations of freshwater fish. Ecotoxicology and Environmental Safety 26, 181–204.

Lemly, A.D., 1997. Ecosystem recovery following selenium contamination in a freshwater reservoir. Ecotoxicology and Environmental Safety 36, 275–281.

Lide, D.R. (Ed.), 1989. CRC: Handbook of Chemistry and Physics, vol. 82. CRC Press, Boca Raton.

Martin, J.M.L., Sundermann, A., 2001. Correlation consistent basis sets for use with the Stuttgart–Dresden–Bonn relativistic effective core potentials: the atoms Ga–Kr and In–Xe. Journal of Chemical Physics 114 (8), 3408–3420.

Miller, B., Dugwell, D.R., Kandiyoti, R., 2003. The influence of injected HCl and SO_2 on the behavior of trace elements during wood-bark combustion. Energy and Fuels 17, 1382–1391.

Mizushima, M., 1972. Molecular parameters of the hydroxyl free radical. Physical Review A: Atomic, Molecular, and Optical Physics 5 (1), 143–157.

Molina, M.J., Molina, L.T., Kolb, C.E., 1996. Gas-phase and heterogeneous chemical kinetics of the troposphere and stratosphere. Annual Review of Physical Chemistry 47, 327–367.

Ohlendorf, H.M., Hoffman, D.J., Saiki, M.K., Aldrich, T.W., 1986. Embryonic mortality and abnormalities of aquatic birds: apparent impacts of selenium from irrigation drainwater. The Science of the Total Environment 52, 59–63.

Pickering, I.J., Prince, R.C., Salt, D.E., George, G.N., 2000. Quantitative, chemically specific imaging of selenium transformation in plants. Proceedings of the National Academy of Sciences of the United States of America (PNAS) 97, 10717–10722.

Senior, C.L., Bool III, L.E., Srinivasachar, S., Pease, B.R., Porle, K., 2000. Pilot scale study of trace element vaporization and condensation during combustion of a pulverized sub-bituminous coal. Fuel Processing Technology 63, 149–165.

Shah, P., Strezov, V., Stevanov, C., Nelson, P.F., 2007. Speciation of arsenic and selenium in coal combustion products. Energy and Fuels 21, 506–512.

Stevens, W.J., Krauss, M., 1992. Relativistic compact effective core potentials and efficient, shared-exponent basis sets for

the third-, fourth- and fifth-row atoms. Canadian Journal of Chemistry 70, 612–630.

Thermodynamics Source Database, 2005. In: Linstrom, P.J., Mallard, W.G. (Eds.), NIST Chemistry Webbook. NIST Standard Reference Database Number 69. Thermodynamic Research Center, NIST Boulder Laboratories, National Institute of Standards and Technology, Gaithersburg.

Tinggi, U., 2003. Essentiality and toxicity of selenium and its status in Australia: a review. Toxicology Letters 137, 103–110.

US Department of Health and Human Services, Agency for Toxic Substances and Disease Registry (ATSDR), 2003. Toxicological Profile for Selenium, 457pp.

Yan, R., Gauthier, D., Flamant, G., 1999. Possible interactions between As, Se, and Hg during coal combustion. Combustion and Flame 120, 49–60.

Yan, R., Gauthier, D., Flamant, G., Peraudeau, G., 2001. Fate of selenium in coal combustion: volatilization and speciation in the flue gas. Environmental Science and Technology 35, 1406–1410.

Yan, R., Gauthier, D., Flamant, G., Wang, Y., 2004. Behavior of selenium in the combustion of coal or coke spiked with Se. Combustion and Flame 138, 20–29.

Young, 1979. United States Patent, 4,142,912.

Zeng, T., Sarofim, A., Senior, C., 2001. Vaporization of arsenic, selenium, and antimony during coal combustion. Combustion and Flame 126, 1714–1724.

Zhang, B., Xu, H., Yu, J.C., 2002. Determination of total gaseous selenium in atmosphere by honeycomb denuder/ differential pulse cathodic stripping voltammetry. Talanta 57, 323–331.